Efficient Approximation of Neural Filters for Removing Quantum Noise From Images

Kenji Suzuki, *Member, IEEE*, Isao Horiba, and Noboru Sugie, *Member, IEEE*

***Abstract*—In this paper, efficient filters are presented that approximate neural filters (NFs) that are trained to remove quantum noise from images. A novel analysis method is proposed for making clear the characteristics of the trained NF. In the proposed analysis method, an unknown nonlinear deterministic system with plural inputs such as the trained NF can be analyzed by using its outputs when the specific input signals are input to it. The experiments on the NFs trained to remove quantum noise from medical and natural images were performed. The results have demonstrated that the approximate filters, which are realized by using the results of the analysis, are sufficient for approximation of the trained NFs and efficient at computational cost.**

***Index Terms*—Analysis method, approximate filter, efficient realization, image enhancement, neural network, signal processing.**

I. Introduction

RECENTLY, significant progress has been made in applying neural networks (NNs) to signal processing. Nonlinear filters based on multilayer NNs, called neural filters (NFs), have been studied. By training the NF with a set of input signals and desired signals, it acquires the function of a desired filter. Two classes of NFs have been proposed so far. One is realized as stack filters [1]; an input signal is transformed into binary signals on the basis of the threshold decomposition, and then, each of them is input to each of plural multilayer NNs. It has been shown in [2]–[10] that the performance of these NFs is excellent in removing impulsive noise from signals/images. The other is a filter where input signals are input directly to a multilayer NN. It has been shown in [11]–[18] that the performance of these NFs is excellent in removing Gaussian/quantum noise from signals/images.

Many studies on the capability of the NFs or the NNs, used as a model of them, have been performed so far; it has been reported that the former class of NFs unifies various nonlinear filters, such as finite impulse response filters, microstatistic filters, generalized weighted order statistic filters, and generalized stack filters [2], [4]–[7], [9]. Relationships between stack filters and the NNs have also been examined in [19] and [20]. The analyses and simulations of the NFs have been reported in [2], although their structures are restricted to a single neuron representing a linear discriminant function. It has been reported in [11] and [12] that epsilon filters, which are nonlinear filters developed for noise removal, are special cases of the latter class of NFs. Furthermore, it has been proved that any continuous mapping can be approximately realized by multilayer NNs [21]–[26]. Thus, the capability of the NFs is getting clearer.

However, the characteristics of the trained NFs have yet to be understood explicitly because to analyze them is difficult due to the complicated structure composed of many units with nonlinear characteristics. For practical use, particularly in the critical applications such as those to medical systems, it is strongly required to make their characteristics clear. However, studies on analyzing the trained NFs have yet to be reported. Furthermore, since the computational cost and the cost of hardware of the NFs are exceedingly high, the reduction is a serious issue for making the NFs practicable. In applications of filters to medical X-ray image sequences, it is required to process 30 frames/s, where each image consists of 1024×1024 pixels $\times 10$ bits. Therefore, how to analyze the trained NF and to reduce the computational cost have remained serious issues.

In this paper, we propose a novel method for analyzing the trained NFs that belong to the latter class to make the characteristics clear and realize their efficient approximate filters using the results of the analysis. In the proposed analysis method, an unknown nonlinear deterministic system with plural inputs such as the trained NF can be analyzed by using its outputs when the specific input signals for analysis are input to it. One of the basic functions of filters for signal/image processing is noise reduction. Quantum noise is signal-dependent noise and is generally observed in photon-limited images such as images obtained in darkness, those obtained by an infrared camera, X-ray images, and so on. We narrow down the issues to the NFs trained to remove quantum noise from images because to analyze the NFs trained to solve various problems is too difficult. Through experiments on the NFs trained to remove quantum noise from medical X-ray image sequences and natural images, the efficiency of both the proposed analysis method and the approximate filter are shown.

II. Neural Filter for Removing Quantum Noise From X-ray Image Sequences

A. Architecture of the Neural Filter

The NF consists of a multilayer NN in which the activation functions of the units in the input, hidden, and output layers are an identity function, a sigmoid function, and a linear function,

Manuscript received June 13, 2000; revised March 1, 2002. This work was supported in part by the Ministry of Education, Science, Sports, and Culture of Japan under a grant-in-aid for quantum information theoretical approach to life science and a grant-in-aid for the encouragement of young scientists. The associate editor coordinating the review of this paper and approving it for publication was Dr. Kenneth Kreutz-Delgado.

K. Suzuki and I. Horiba are with the Faculty of Information Science and Technology, Aichi Prefectural University, Aichi, Japan.

N. Sugie is with the Faculty of Science and Technology, Meijo University, Nagoya, Japan.

Publisher Item Identifier S 1053-587X(02)05645-3.

respectively. We adopted a linear function instead of an ordinarily used sigmoid one as the activation function of the unit in the output layer because the characteristics of the NN become better in the applications to continuous mapping issues such as image processing [27], [28]. The inputs to the NF are an object pixel value and spatially/spatiotemporally adjacent pixel values. We explain, as an example, a three-layered spatiotemporal NF [13], [15]. The architecture of the NF is shown in Fig. 1. In Fig. 1, t_0 and T denote a time of the current frame and a time interval between frames, respectively. The output of the NF is represented by

$$f(x,y,t) = G_M \cdot NN\left(\boldsymbol{I}_{x,y,t}\right) \tag{1}$$

where

$$\boldsymbol{I}_{x,y,t} = \left\{ \frac{g(x-i,y-j,t-k)}{G_M} | i,j,k \in R \right\} \tag{2}$$

denotes the input vector to the NF, and

x and y	indices of spatial coordinates;
t	index of temporal coordinate;
$g(x,y,t)$	pixel value in the input image;
$NN(\boldsymbol{I})$	output of the multilayer NN;
G_M	normalization factor;
R	input region of the NF.

The input vector is rewritten as

$$\boldsymbol{I}_{x,y,t} = \{I_1, I_2, \ldots, I_m, \ldots I_{N_I}\} \tag{3}$$

where m denotes a unit number in the input layer and N_I the number of units in the input layer. As the activation function of the units in the input layer is an identity function $f_I(\cdot)$, the output of the mth unit in the input layer is represented by

$$O_m^I = f_I\left(I_m\right) = I_m. \tag{4}$$

The output of the hth unit in the hidden layer is represented by

$$O_h^H = f_S\left\{ \sum_{m=1}^{N_I} \left(W_{mh}^H \cdot O_m^I\right) - W_{0h}^H \right\} \tag{5}$$

where

W_{mh}^H	weight between the mth unit in the input layer and the hth unit in the hidden layer;
W_{0h}^H	offset of the hth unit in the hidden layer;
N_H	number of units in the hidden layer;
$f_S(u)$	sigmoid function

$$f_S(u) = \frac{1}{1+\exp(-u)}. \tag{6}$$

The output of the unit in the output layer is represented by

$$NN\left(\boldsymbol{I}_{x,y,t}\right) = f_L\left\{ \sum_{h=1}^{N_H} \left(W_h^O \cdot O_h^H\right) - W_0^O \right\} \tag{7}$$

where

W_h^O	weight between the hth unit in the hidden layer and the unit in the output layer;
W_0^O	offset of the unit in the output layer;

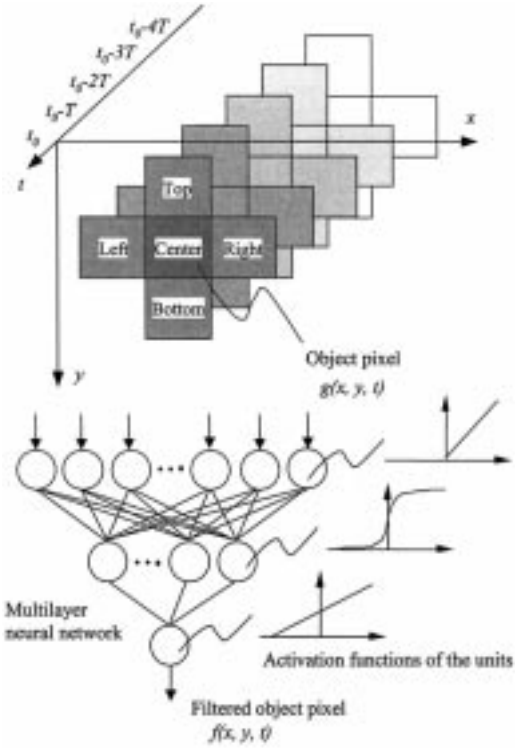

Fig. 1. Architecture of the neural filter (NF) for image sequence processing.

$f_L(u)$	linear function

$$f_L(u) = u + \frac{1}{2}. \tag{8}$$

The error to be minimized by training is defined as

$$E = \frac{1}{P} \sum_p \left(\frac{T_C^p}{G_M} - \frac{f^p}{G_M} \right)^2 \tag{9}$$

where

p	pattern number;
T_C^p	pth pattern in the teaching image;
f^p	pth pattern in the output image;
P	number of patterns.

The NF is trained by the backpropagation algorithm [29] until the error E gets smaller than or equal to the predetermined error E_P or the number of training epochs exceeds the predetermined number T_P. By using this training algorithm, it is expected that the NF would have the function to convert the input image to the desired teaching image, e.g., by presenting the noisy input image together with the teaching noiseless image, details of which are clear, and that the NF will be able to remove noise from images while preserving image details.

B. Synthesizing Input and Teaching Images

Medical X-ray images are treated in this section because the analysis of novel technologies such as the NFs is very important, particularly in the applications to medical systems. The goals of improving the image quality of medical X-ray image sequences are 1) to remove quantum noise from low-dose X-ray images to reduce X-ray exposure to patients and 2) to enhance the edges in diagnostic regions in the images to discern them clearly.

X-ray quantum noise is originated from a signal-dependent Poisson-distributed noise source [30]. The variance of the Poisson noise increases linearly with signal amplitude, i.e., local X-ray exposure. However, the signal-to-noise ratio (SNR) increases with X-ray exposure. Since in most X-ray systems the mean brightness is controlled by an automatic gain control (AGC) in order to make it a constant brightness, the observed quantum noise decreases with increasing X-ray exposure [31]. Using this property, the input and teaching images for training can be synthesized from high-dose X-ray images taken at a high X-ray exposure level.

The low-dose X-ray image $g_L(x,y,t)$, which is the input image to the NF, can be synthesized from the high-dose X-ray image with negligible quantum noise $g_H(x,y,t)$ as

$$g_L(x,y,t) = g_H(x,y,t) + X_N(\sigma) \tag{10}$$

$$\sigma = k_N\sqrt{g_H(x,y,t)} \tag{11}$$

where $X_N(\sigma)$ denotes white Gaussian noise when its standard deviation is σ, and k_N is the parameter determining the amount of radiation dosage. In clinical examinations, the X-ray image sequence is acquired at very low X-ray dose: Only ten to 500 X-ray quanta contribute to each pixel [32]. The average number of X-ray quanta captured at one pixel is about 35 [30], [33]. The Poisson-distributed noise can be approximated by the Gaussian one when the number of X-ray quanta is more than 20 [34]. Therefore, we can use the Gaussian noise as a model of the quantum noise.

Moving low-dose X-ray images such as fluoroscopic images and radiographs are generally inverted to make them look like traditional film negatives. If the acquired high-dose X-ray image is inverted, we need to invert the gray levels of the image before synthesizing. Furthermore, most of medical imaging systems use a signal-dependent gain, e.g., in fluoroscopic imaging systems, called white compression (or white suppression); this measure is taken to prevent halation. In digital radiography systems, a logarithmic gain curve is sometimes used. In such a case, we need to perform the inverse transformation of the white compression and/or the logarithmic gain curve on the high-dose X-ray image before synthesizing the input and the teaching images.

The spatial frequency characteristic of quantum noise depends on that of an acquisition system. If we use a camera tube-based acquisition system, the modulation transfer function (MTF) of quantum noise is a bell shape. If we use a CCD-based acquisition system, the shape of the MTF becomes more flat. Thus, the actual spatial frequency characteristic of quantum noise is not white but depends on that of the acquisition system. We adopted a simpler model because one of issues of this paper is efficient realization of the NF. If we adopt a complex model, the analysis may become more complex. However, using a stricter model would lead to improvement of the performance of the NF, especially in applications to medical X-ray images (see the detailed properties of the actual medical X-ray imaging system in [31] to construct a stricter model).

The teaching image $T_C(x,y,t)$ is synthesized from $g_H(x,y,t)$ by performing a highpass filtering, the window function of which is represented by (12), shown at the bottom of the page, where

- u normalized horizontal spatial frequency;
- v normalized vertical spatial frequency;
- f_C parameter determining the passband.

We obtained k_N of 0.24% of the maximum gray level by the actual measurement of noise in low-dose X-ray images [35] and used f_C of 1/16.

C. Training the Neural Filter

The spatiotemporal input region of the NF consists of five pixels $[(x,y-1),(x-1,y),(x,y),(x+1,y),(x,y+1)]$ in each of five consecutive frames, as Fig. 1 shows. We adopted three-layered NF because it has been proved theoretically that any continuous mapping can be approximately realized by three-layered NNs [21], [22]. The number of units in the input, hidden, and output layers are 25, 20, and 1, respectively (here referred to as 25-20-1). The number of units in the hidden layer was determined by trial and error. The experimental results showed that 20 units are enough to train the NF for quantum noise removal.

The images used for training are shown in Fig. 2. These are radiographs of a stomach (size: 512×512 pixels; number of gray levels: 1024) called a double contrast radiograph, which was acquired with a digital radiography system. These images were inverted to make them look like traditional film negatives. In these figures, a 70×120-overlay shows a region of interest that was enlarged to double the original size. The high-dose X-ray images were acquired at a high X-ray exposure level based on a common dose protocol used in radiography. The simulated low-dose X-ray images $g_L(x,y,t)$, synthesized from the high-dose X-ray images by using (10), are shown in Fig. 2(a) and (b). In the figures, the current and the last frame in the input region of the NF are shown. The peristaltic movement of the stomach wall can be seen by comparing between Fig. 2(a) and (b). The inverse transformation of the logarithmic gain curve was performed on the high-dose X-ray image $g_H(x,y,t)$ before synthesizing. All images in Fig. 2 are displayed as the image after performing the inverse transformation because the double contrast radiograph is often displayed this way. The teaching image $T_C(x,y,t_0)$, which is synthesized from the high-dose X-ray image, is shown in Fig. 2(c). These kinds of images are used for the medical examination of stomach cancer. Through training with these images, the NF would acquire the function of noise reduction as well as edge enhancement. The NF was trained on 80 000 epochs with the training set in the regions indicated by the white rectangular frames (90×60 pixels) in Fig. 2.

$$P_H(u,v) = \begin{cases} \frac{3}{2} + \frac{1}{2}\cos\left(\pi\frac{f_C - \sqrt{u^2+v^2}}{f_C}\right) & \left(0 \le \left|\sqrt{u^2+v^2}\right| \le f_C\right) \\ 2 & \left(f_C \le \left|\sqrt{u^2+v^2}\right| \le \frac{1}{2}\right) \end{cases} \tag{12}$$

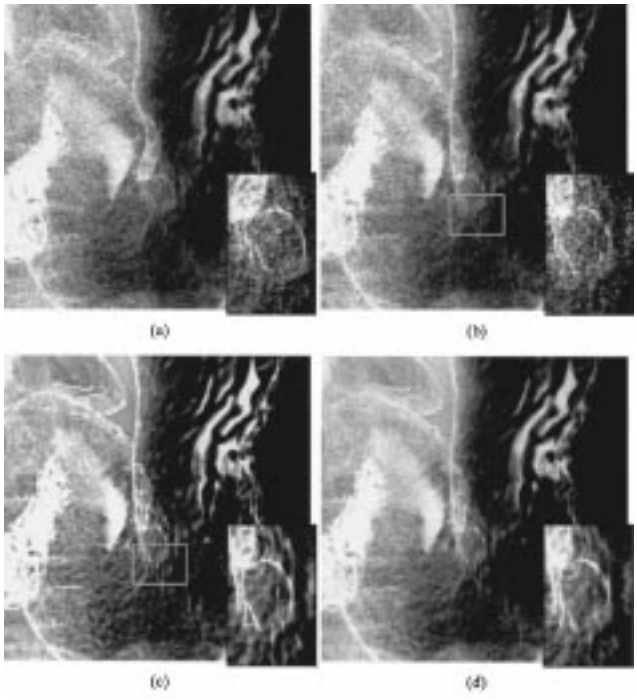

Fig. 2. Images used for training and the output image of the trained NF. (a) Simulated low-dose X-ray image, the last frame in the input region of the NF $g_L(x, y, t_0 - 4T)$. (b) Simulated low-dose X-ray image, the current frame in the input region of the NF $g_L(x, y, t_0)$. (c) Teaching image synthesized from a high-dose X-ray image $T_C(x, y, t_0)$. (d) Output image of the trained NF. White rectangular frames in (b) and (c) indicate the training region.

We selected such a small region as the training region because the features in a smaller region would be easier to analyze. Using a wider training region would make the NF much more versatile. The training converged with the error E of 0.024.

The output image of the trained NF is shown in Fig. 2(d). The noise in the input images is reduced, and the edges become sharper. The noise reduction and edge enhancement, which are adapted to the training region, are achieved, although the quality of the image does not reach the teaching image.

In general, there is a risk occurring of artifacts in filtering image sequences using a spatiotemporal input region. Data in the previous frame may appear in the current frame. There is a tradeoff between the filter performance and the risk in designing filters. The balance between the two is important in filter design. The NF can be designed to balance the risk with the performance, i.e., since the NF is trained with image sequences in order that the output image approaches the teaching image that contains no artifact, the weights yielding artifacts would diminish through training. However, the training is not completed with the error of zero. Therefore, there still remains a risk of reappearing features of previous frames with the trained NF. Thus, analyzing the trained NF is of importance. If the trained NF is analyzed, we can know a risk and may have a way to reduce it.

III. Analysis Method for the Trained Neural Filter

A. Specific Input Signals for Analysis

We have reported the preliminary version of the proposed method in [36]. If a system is a linear system, it can be analyzed clearly by using its impulse response. However, it is difficult to analyze theoretically the NFs trained to solve various problems because of their nonlinearity. We narrow down the issues to the NF trained to remove quantum noise from images. Since the quantum noise is signal dependent, the NF trained to remove it should be realized with the characteristics depending on gray levels in the images. Furthermore, the trained NF can be treated as a nonlinear deterministic system. By paying attention to these points, the trained NF can be analyzed experimentally; an unknown nonlinear deterministic system such as the trained NF would be analyzed by using its output responses that are obtained when some input signals for analysis are input to it.

Since the NF is a system that has a lot of inputs, as a practical matter, all possible combinations of input signals cannot be tested. Therefore, we need to generate input signals on the basis of some rule. As described above, the characteristics of the NF trained to remove quantum noise would depend on the average gray level in the input region. Let us suppose that the same gray level is input to all input units, except a certain target-input unit. In such a case, the same gray level approximately corresponds to the local average gray level. If we adopt a rule that only the gray level to the target-input unit is varied, we can obtain the output response to the target-input unit around the local average gray level. Thus, we can analyze a nonlinear system with plural inputs, which is represented by the model having the local average gray level as a parameter.

The specific input signals for analysis are defined as

$$\forall m\, I_{m,D}(s) = \begin{cases} s, & \text{if } m = q \\ D, & \text{if } m \neq q \end{cases} \quad (0 \leq s \leq 1) \tag{13}$$

$$\forall q, D\, \boldsymbol{I}_{q,D} = \{I_{1,D}, I_{2,D}, \ldots, I_{q,D}, \ldots, I_{N_I,D}\} \tag{14}$$

where

- m unit number in the input layer ($1 \leq m \leq N_I$);
- D base signal ($0 \leq D \leq 1$);
- s parameter ($0 \leq s \leq 1$);
- q target-input unit number ($1 \leq q \leq N_I$).

As is shown in Fig. 3, the output response to a certain target-input unit is examined. The ramp signal with respect to the parameter s is input to the target-input unit q; the base signals D, which are constant values with respect to s, are input to the other input units. Furthermore, in order to examine the output responses to the base signals D, the value of D is varied between zero and one. By changing the target-input unit from one to another, the output responses to all of the input units are examined. The output response of the NF to q and D is represented by

$$O_{q,D}(s) = NN\left(\boldsymbol{I}_{q,D}(s)\right). \tag{15}$$

Thus, in the proposed analysis method, the output response to a target-input unit is obtained like a sensitivity analysis method. After the sensitivities, i.e., the output responses, of all input units are obtained, the NF can be represented by some model.

B. Approximate Filter Model

Consider the filter model represented by

$$O = \sum_{m=1}^{N_I} F_{m,D}\left(I_m\right) \tag{16}$$

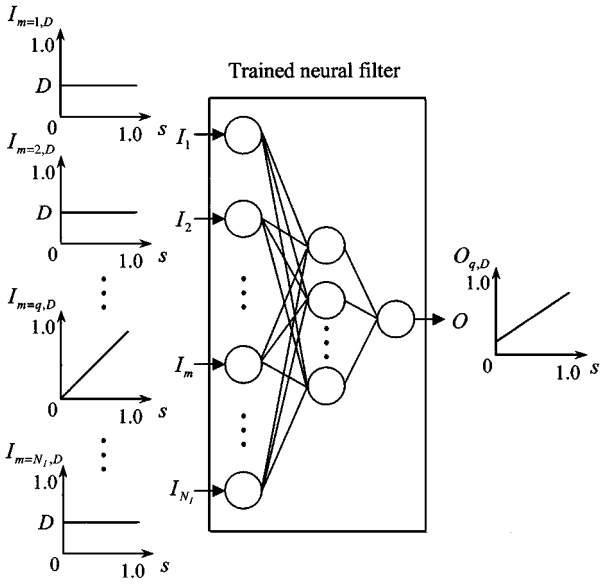

Fig. 3. Analysis method for unknown nonlinear deterministic systems such as trained NFs.

where $F_{m,D}(I_m)$ denotes a polynomial of degree N represented by

$$F_{m,D}\left(I_m\right) = \sum_{n=0}^{N} a_{m,D}^{(n)} \cdot I_m^n \tag{17}$$

where $a_{m,D}^{(n)}$ denotes a filter coefficient, and n refers to a parameter. By substituting (13) into (14), the input vector to the filter model is represented by

$$\boldsymbol{I}_{q,D}(s) = \{D, D, \ldots, s, \ldots D\}. \tag{18}$$

Substituting the parameter s for $I_{q,D}$, we obtain the output response of the filter model to q and D, to which the specific input signals for analysis are input, as

$$O_{q,D}\left(I_{q,D}\right) = \sum_{n=0}^{N} a_{q,D}^{(n)} \cdot I_{q,D}^n + \sum_{m \neq q}^{N_I} \left\{ \sum_{n=0}^{N} a_{m,D}^{(n)} \cdot D^n \right\}. \tag{19}$$

Applying the least-squares method to the approximation of the output responses, the filter coefficients $a_{m,D}^{(n)}$ can be obtained.

Let us now assume that the degree N is equal to one. The filter model becomes simple, as the following equation shows:

$$O = \sum_{m=1}^{N_I} \left\{ a_{m,D}^{(1)} \cdot I_m + a_{m,D}^{(0)} \right\}. \tag{20}$$

By replacing $a_{m,D}^{(1)} \equiv a_m(D)$ and $\sum_{m=1}^{N_I} a_{m,D}^{(0)} \equiv b(D)$, the output response of the filter model to q and D can be represented by

$$O_{q,D}\left(I_{q,D}\right) = a_q(D) \cdot I_{q,D} + \sum_{m \neq q}^{N_I} a_m(D) \cdot D + b(D) \tag{21}$$

where $a_m(D)$ and $b(D)$ denote the filter coefficients depending on D. By applying the least-squares method to the approximation, the filter coefficients $a_m(D)$ and $b(D)$ can be obtained. By this approximation, as well as approximating the base signal D to the summation of the inputs, we obtain the approximate filter model represented by

$$O = \sum_{m=1}^{N_I} a_m\left(N_I \cdot D\right) \cdot I_m + b\left(N_I \cdot D\right) \tag{22}$$

where $a_m(\cdot)$ and $b(\cdot)$ are implemented as look-up tables with the summation of the inputs $N_I \cdot D$ as an index. The last equation gives the approximate filter model shown in Fig. 4. The hardware architecture is very simple. It consists of multipliers, adders, and table memories; it is like a transversal filter, apart from the nonlinearity of the table memories.

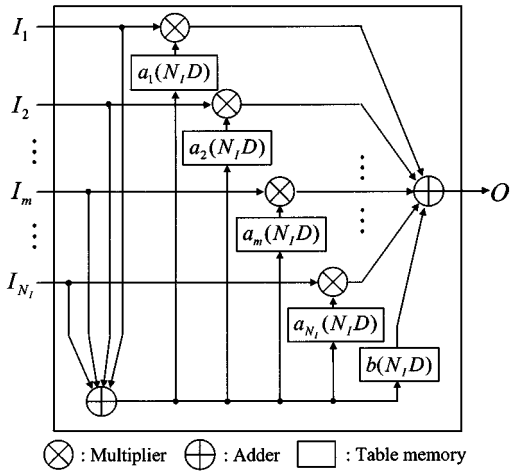

Fig. 4. Hardware architecture of the approximate filter.

In the NF, since multiplications of the signals by the weights are dominant over other operations, the computational cost of the NF is proportional to the number of multiplications. The number of multiplications of the NF can be derived as

$$N_C = N_H\left(N_I + 1\right). \tag{23}$$

In contrast, the number of multiplications of the approximate filter model in case of the degree N is represented by

$$N_C = N_I(2N - 1). \tag{24}$$

Therefore, the approximate filter is advantageous in terms of the computational efficiency when the following condition is fulfilled:

$$N_I(2N - 1) < N_H\left(N_I + 1\right). \tag{25}$$

If the NF can be approximated accurately by the approximate filter in case of the degree N of one, i.e., the approximate filter shown in Fig. 4, the number of multiplications corresponds to the number of units in the input layer as

$$N_C = N_I. \tag{26}$$

Therefore, the computational cost of the NF is reduced to about $1/N_H$ in the case where the trained NF can be approximated by the approximate filter shown in Fig. 4.

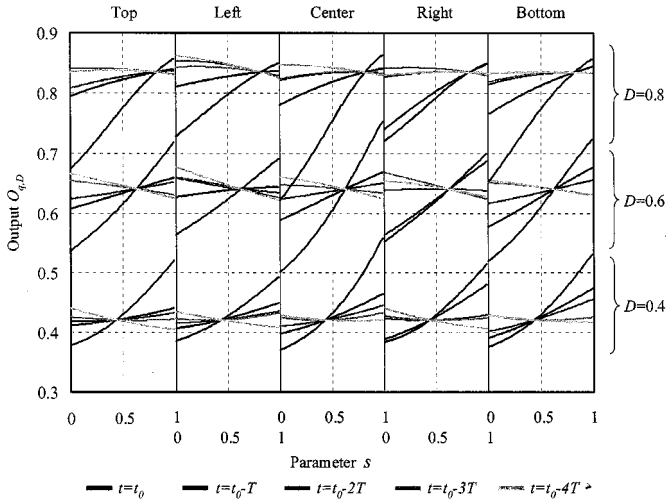

Fig. 5. Output responses of the trained NF to which the specific input signals for analysis are input.

IV. Experiments

A. Results of Analysis and Realizing the Approximate Filter

The proposed analysis method was applied to the NF trained to improve the image quality of medical X-ray image sequences. The output responses of the trained NF, to which the specific input signals for analysis are input, are shown in Fig. 5. In Fig. 5, the output responses are shown for D equal to 0.4, 0.6, and 0.8. The words Top, Left, Center, Right, and Bottom express spatial positions of the input region of the NF shown in Fig. 1. The brightness of curves corresponds to the temporal position of the frame in the input region, similar to the fading brightness of the pixels in Fig. 1. A black curve indicates the current frame, and a brighter curve indicates an older frame. The gradient of each curve expresses a nonlinear filter gain at the corresponding input unit. The pixel having the same sign of the gradient as the sign at the object pixel, i.e., the pixel at the position Center in the current frame t_0, indicates that the pixel has averaging effect. The pixel having the opposite sign indicates that the pixel has spatial/temporal edge enhancement effect. An intersection point of curves indicates the output response when all input signals are the same.

Since all of the output responses are nearly straight, they can be approximated by linear functions well, i.e., there is a possibility that this trained NF can be approximated by the approximate filter model, the degree of which is equal to one, in (21). We applied the least-squares method to the approximation of the output responses to linear functions. The mean absolute error between the output responses and linear functions was calculated in order to examine the accuracy in approximation. As a result, the mean absolute error was only 2.05%. This result indicates that the degree of one is enough to approximate this trained NF. Therefore, this trained NF can be approximated by the approximate filter shown in Fig. 4.

Abdominal radiographs are acquired at a speed up to 30 frames/s, where each image consists of 1024×1024 pixels $\times 10$ bits. The previously discussed 25-20-1 NF requires 520 multiplications per pixel. Consequently, real-time filtering of abdominal images would require 16.4 billion multiplications per second. By using the approximate filter, the cost of hardware of the NF is reduced to about 1/20. According to (25), the approximate filter in case where the degree N is less than or equal to ten is advantageous in terms of the computational efficiency. We can chose the appropriate degree N, according to the accuracy required by its application. In general, if we use the approximate filter model including the higher order terms and their mixed terms, the approximation would be more robust and accurate.

Figs. 6 and 7 show the results of calculation of the filter coefficients of the approximate filter obtained from the output responses. The gradient of the line approximating the curve in Fig. 5 corresponds to the filter coefficient $a(D)$ at the corresponding position in the corresponding frame, e.g., since the gradient of the line at the object pixel in case where D equals to 0.6 in Fig. 5 is about 0.24, the filter coefficient $a(D = 0.6)$ at the object pixel is about 0.24. Since the gradients of some lines in older frames are negative, the corresponding filter coefficients $a(D)$ in the older frames are negative.

The filter coefficients at the center pixels Fig. 6(c) are relatively greater than those at the other pixels. The same sign of a filter coefficient as the sign of the filter coefficient at the object pixel indicates the averaging effect. This effect would reduce quantum noise adapting to the gray level. The filter coefficients decrease in proportion to the temporal distance from the current frame t_0. This characteristic is due to the training to process time-varying images. They are negative in the frames $t_0 - 3T$ and $t_0 - 4T$. This indicates that the edge enhancement is mainly performed in these frames. Since these negative coefficients may cause an artifact in the case of motion, we need to perform a subjective evaluation with specialists to confirm the occurrence of no artifact (the results of the subjective evaluation will be shown in the latter section). If any artifact-disturbing clinical diagnosis is observed, we have to reduce the artifact by making the negative coefficients smaller, for example. The filter coefficients in the middle of D are relatively greater than the others. This is caused by the gray-level histogram in the training region; the frequencies around the middle of gray levels are relatively high, as Fig. 8 shows. Furthermore, the filter coefficients at the Top and Bottom are relatively greater than are those at the Left and Right. This is due to the fact that the training region shown in Fig. 2 contains mainly vertically directional patterns. This indicates that the characteristics are adapted to the training region. This fact suggests that it is better to use a wider region as a training region for practical use. Using a wider training region would make the NF, as well as the approximate filter, much more versatile.

Furthermore, the sensitivity of the unit in the input layer can be analyzed by using the filter coefficients. The sensitivity of the mth unit in the input layer is defined as

$$S_m = \frac{\int |a_m(D)|\, dD}{N_D} \tag{27}$$

where N_D denotes a normalization factor. The result of calculation is shown in Fig. 9. The sensitivity of the object pixel is the highest of all. The sensitivity decreases in proportion to the distance from the center pixel in the current frame. This characteristic is due to the training to process time-varying images.

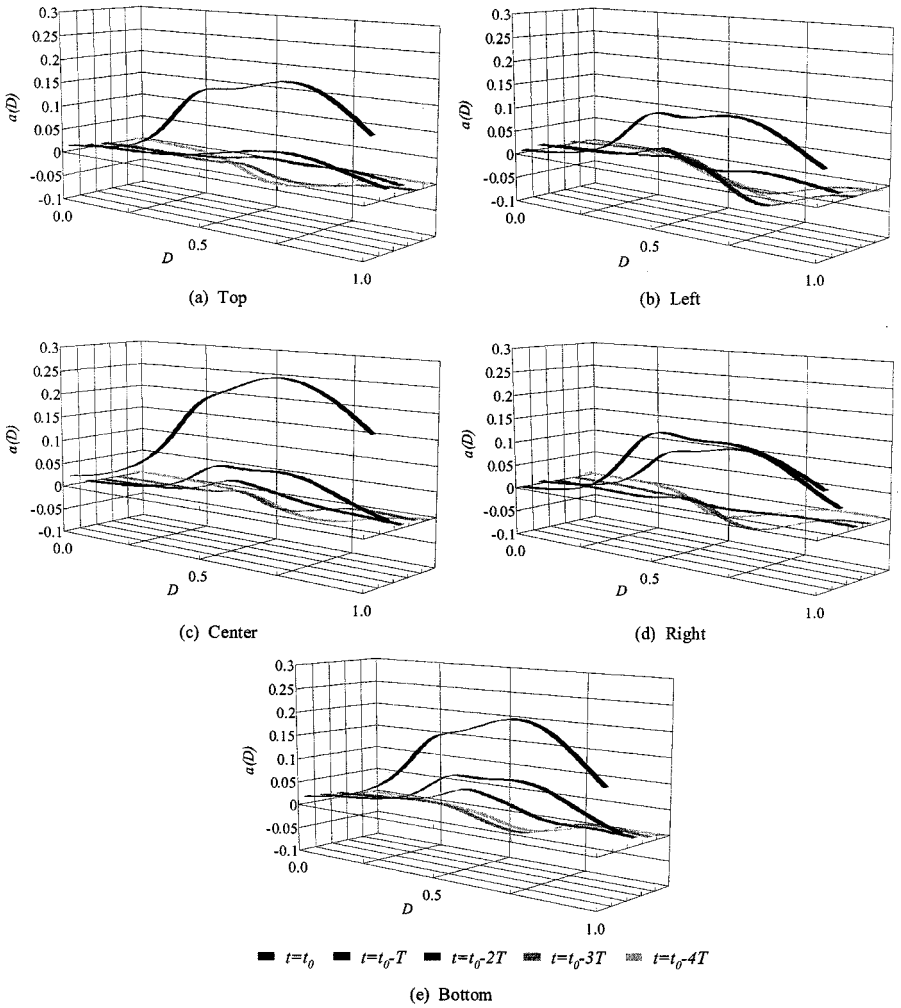

Fig. 6. Results of calculation of the filter coefficients of the approximate filter $a_m(D)$.

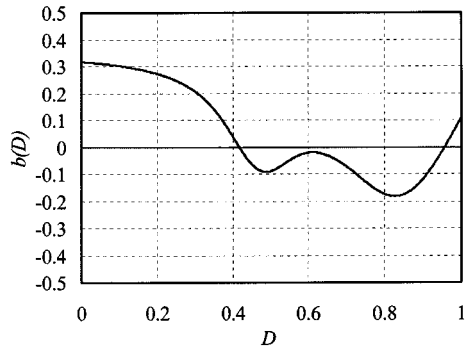

Fig. 7. Results of calculation of the filter coefficient of the approximate filter $b(D)$.

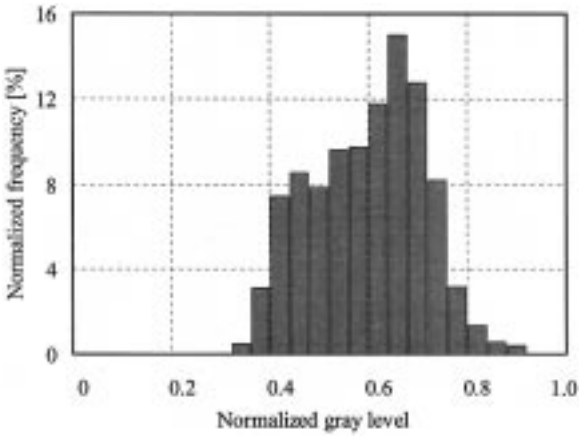

Fig. 8. Histogram of gray level in the training region.

B. Accuracy in Approximation

The accuracy in approximation between the trained NF and its approximate filter is evaluated. First, the output image of the NF and that of the approximate filter are compared. These are shown in Fig. 10(a) and (b). In both images, the noise in the input images is reduced effectively, and the edges become sharper. At first sight, the difference between them cannot be distinguished. To compare more precisely, the image quality is evaluated quantitatively using the blurred signal-to-noise ratio (BSNR) and the improvement in signal-to-noise ratio (ISNR) [37], [38]. These metrics are often used to evaluate image restoration techniques that restore the images degraded by blurring and noise. The

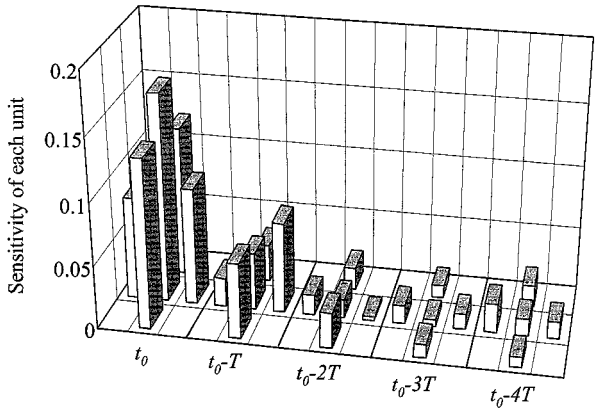

Fig. 9. Results of calculation of the sensitivity of each unit in the input layer.

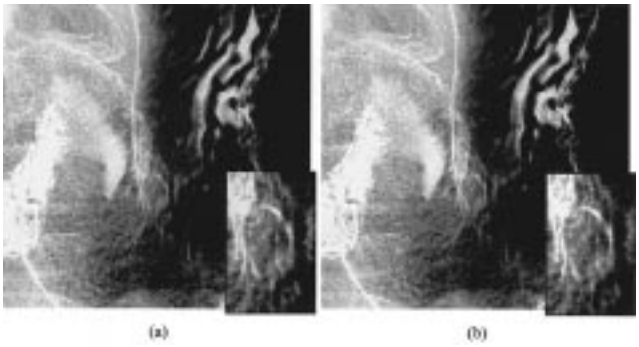

Fig. 10. Comparison of image quality between the output image of the trained NF, whose structure is 25-20-1 and that of its approximate filter. (a) Output image of the trained NF. (b) Output image of the approximate filter.

BSNR and the ISNR are defined as

$$\mathrm{BSNR}(t) = 10\log_{10}\frac{\sum_{x,y\in R_E}\left\{g_H(x,y,t)-\overline{g_H(x,y,t)}\right\}^2}{\sum_{x,y\in R_E}\left\{Ns(x,y,t)-\overline{Ns(x,y,t)}\right\}^2} \tag{28}$$

where

$$Ns(x,y,t) = g_L(x,y,t) - g_H(x,y,t) \tag{29}$$

and where

R_E	region for evaluation;
$\overline{Ns(x,y,t)}$	noise in the input image;
$\overline{T_C(x,y,t)}$	spatial average value within R_E in $T_C(x,y,t)$;
$\overline{Ns(x,y,t)}$	spatial average value within R_E in $Ns(x,y,t)$;

and

$$\mathrm{ISNR}(t) = 10\log_{10}\frac{\sum_{x,y\in R_E}\{T_C(x,y,t)-g_L(x,y,t)\}^2}{\sum_{x,y\in R_E}\{T_C(x,y,t)-f(x,y,t)\}^2}. \tag{30}$$

The results are shown in Fig. 11. R_E was set to the region including whole of the stomach. The average BSNR, i.e., the SNR of the input image, is 11.6 dB. The average ISNR of the NF is 1.866 dB, after using only one frame (number 15) in the training.

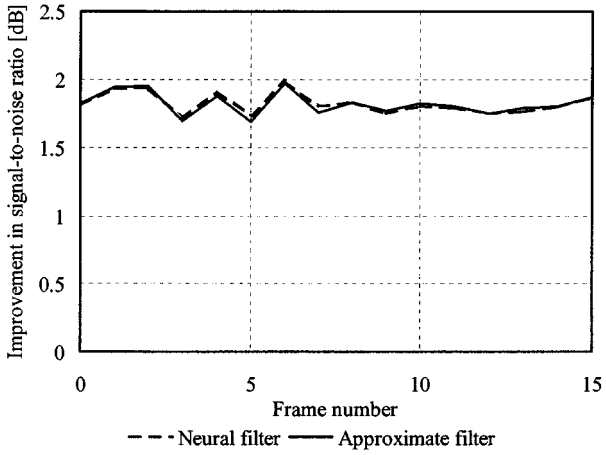

Fig. 11. Comparison of the performance of the trained NF, whose structure is 25–20–1, with that of its approximate filter in terms of the ISNR.

We do not need the entire sequence for training. The average ISNR of the approximate filter is 1.866 dB. The ISNR of the approximate filter is nearly equal to that of the NF in not only the training frame but also the nontraining ones. This result shows that the approximate filter is a very good approximation of the trained NF.

C. Experiments to Verify the Versatility

1) Neural Filter With Large Input Region: In order to evaluate the versatility of the proposed analysis method, an experiment on the NF with a large input region was performed. The input region of the NF is expanded to that consisting of five-by-five pixels in the consecutive five frames. The numbers of units in the input and hidden layers are 125 and 20, respectively. The output image of the trained large NF is shown in Fig. 12(a). As the input region is expanded, the noise is reduced much more, and the edges are sharper than those in the output image of the small NF. The trained large NF was analyzed by using the proposed analysis method, and then, its approximate filter was obtained. The output image of the approximate filter is shown in Fig. 12(b). At first sight, the difference between them cannot be distinguished. The results of calculation of the ISNR are shown in Fig. 13. The average ISNRs of the approximate filter and the NF are 6.826 and 6.823 dB, respectively. This result shows that the proposed analysis method does function well in the case of the expanding input region.

In order to improve the quality of image sequences, various dynamic filters have been proposed so far [39]–[48]. A real-time system for fluoroscopic filtering has been developed and applied to gastrointestinal studies [45]. A matched filter-type algorithm has been developed to optimize the SNR of the contrast signal in an angiographic image sequence [40]. The hardware of a recursive temporal filter has been developed [39], [41]. A spatiotemporal filtering technique with object detection has been developed to reduce noise while minimizing motion and spatial blur [48]. Stochastic temporal filtering techniques have been developed to enhance fluoroscopic images [46], [47]. We compared the NF with the adaptive weighted averaging filter (AWAF) [43]. The AWAF is developed for noise suppression in

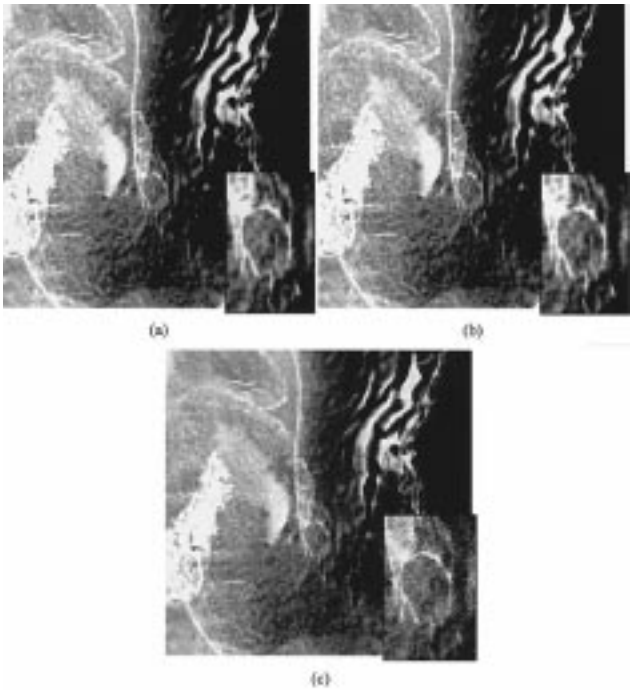

Fig. 12. Comparison of image quality between the output image of the trained large NF, whose structure is 125–20–1 and that of its approximate filter. (a) Output image of the trained large NF. (b) Output image of the approximate filter. (c) Output image of the AWAF.

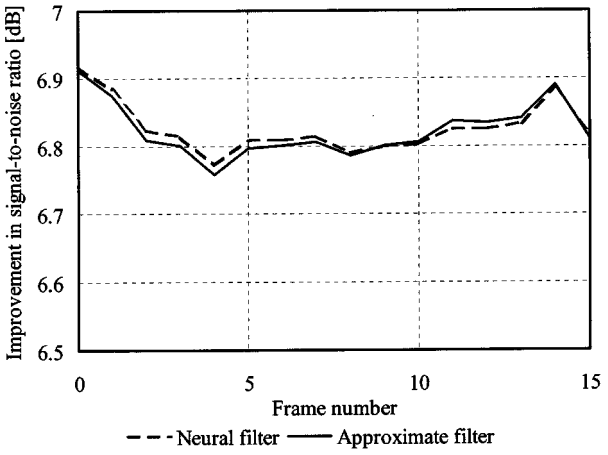

Fig. 13. Comparison of the performance of the trained large NF, whose structure is 125–20–1, with that of its approximate filter in terms of the ISNR.

image sequences without spatial blur. This is the well-known representative as a dynamic filter with good performance. To compare fairly, the input region of the AWAF was set to the same size of the NF; the highpass filtering that was used to synthesize the teaching image for the NF was performed on the output image of the AWAF. The image processed by the AWAF is shown in Fig. 12(c). There remains much noise in the processed image. We cannot discern well the folds of the stomach wall due to the noise. In these kind of images, the fold of the stomach wall is extremely important because medical doctors diagnose stomach cancer on the basis of the convergence pattern of the folds. The average ISNR of the AWAF is 1.3 dB. It is relatively lower because the AWAF would not be developed

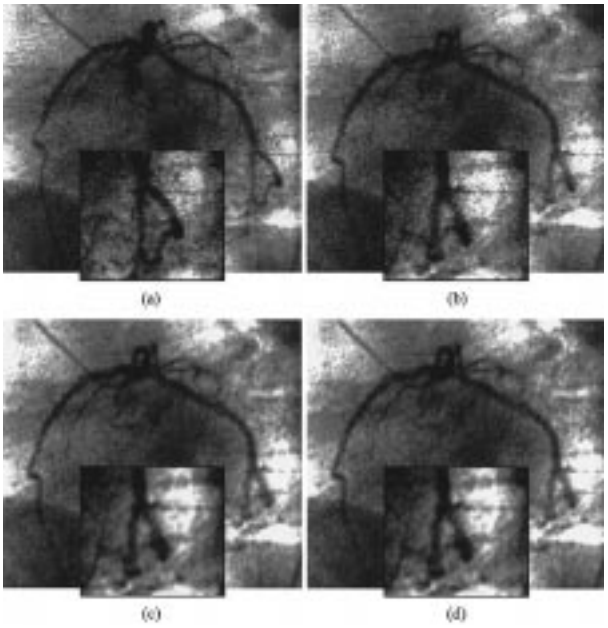

Fig. 14. Comparison of image quality between the output image of the trained large NF, whose structure is 125–20–1, and that of its approximate filter in filtering real low-dose X-ray angiograms, which are not used for training. (a) Last frame in the input region of the NF $g_L(x, y, t_0 - 4T)$. (b) Current frame in the input region of the NF $g_L(x, y, t_0)$. (c) Output image of the trained large NF. (d) Output image of the approximate filter.

for removing the quantum noise in abdominal radiographs. In contrast, in the output images of the NF and the approximate filter, there remains less noise, and we can discern the folds of the stomach wall better.

To compare the computational costs, the CPU execution times of the filters were measured on a workstation (CPU: UltraSparc-II 300 MHz, Sun microsystems). The results of the NF, the approximate filter, and the AWAF are 24.1, 3.7, and 37.6, respectively. The results show that the approximate filter is efficient in computational cost. According to (23) and (26), the computational cost reduction is about $1/N_H$, i.e., 1/20 in this case. However, the actual execution time does not reach it because there is some overhead in software.

2) Evaluation With Real Low-Dose X-ray Images: Apart from abdominal radiography, coronary X-ray angiography is commonly used in medical practice. Both methods have in common that images are acquired at rates up to 30 frames/s. In addition, since the NFs were trained using the simulated low-dose X-ray images, evaluation with real low-dose X-ray images is of importance. Accordingly, the approximate filter was applied to real low-dose angiograms of coronary arteries. The angiograms are shown in Fig. 14(a) and (b). These angiograms were actually acquired at a low X-ray exposure level in clinical X-ray fluoroscopy, i.e., a common low-dose protocol in fluoroscopy was used (the tube current and the tube voltage of the X-ray tube were 1.6 mA and 58 kV, respectively). Although there are many factors in the imaging chain that affect the overall image quality, the noise power attributed to quantum noise dominates the whole noise power at lower spatial frequencies in a low-dose scenario such as X-ray fluoroscopy [49]. The real low-dose X-ray images used in this experiment should dominate low spatial frequency quantum noise.

TABLE I
QUANTITATIVE EVALUATION OF THE ACCURACY IN APPROXIMATION BETWEEN THE TRAINED NF AND ITS APPROXIMATE FILTER

Structure of NF	Image	MAE [%]	RMSE [%]
25–20–1	DCR	0.278	0.453
125–20–1	DCR	0.187	0.255
	ACA	0.200	0.260

DCR : Double contrast radiograph

ACA : Angiogram of coronary artery

The output image of the NF is shown in Fig. 14(c). Since, in a cardiac imaging system, a nonlinear gray level transformation is performed prior to storage, the compensation of the nonlinear transformation was performed before filtering. In the image, the quantum noise is reduced effectively. We can see the arteries better. However, if we use the images, including the low spatial frequency quantum noise for training the NF, the image quality would be much better. Furthermore, in the output image, we can see no artifacts caused by data in the previous frame, although the arteries move quite rapidly. This would be due to the fact that the rapid movement of the stomach wall is partially contained in the images used for training. If no rapid movement was contained in the images used for training, the artifacts might occur in the output image.

In order to evaluate the image quality for clinical use, we performed a subjective evaluation with cardiologists. The evaluation was performed using a real digital angiography system in a hospital. The processed image sequences were loaded into the system and were displayed under the same conditions as in common clinical use. By the evaluation, it was confirmed that there was no artifact-disturbing diagnosis, such as the artifact caused by reappearing features of the previous frames, in the images.

The output image of the approximate filter is shown in Fig. 14(d). The difference between the output image of the NF and that of the approximate filter cannot be distinguished. Furthermore, we performed a subjective evaluation with cardiologists. By the evaluation, it was confirmed that there was no difference between the two in terms of clinical use. This shows that the approximate filter functions well in filtering real low-dose angiograms, which are the different kind of images from the training images. The mean absolute errors between the output images of the NFs and those of the approximate filters are summarized in Table I. The errors in all cases are quite small. This result leads to the conclusion that the approximate filter has enough versatility to apply it to medical systems.

D. Neural Filter Trained to Remove Quantum Noise From Natural Images

In order to evaluate the versatility of the proposed analysis method, an experiment on the NF trained to remove quantum noise from two-dimensional natural images was performed. Since the target image is static, we adopted the spatial region as the input region of the NF. In order to reduce noise sufficiently, the spatial input region of the NF was set to that consisting of 11×11 pixels. The number of units in the input and hidden layers are 121 and 50, respectively. The image used in this experiment is the Lena image (size: 512×512 pixels; number of gray levels: 256) from the University of Southern California image database. Fig. 15(a) and (b) shows the noisy input image synthesized by using (10) and the teaching image, respectively. k_N was set to 5% of the maximum gray level. In order to acquire the features in the entire image, the training set is made by sampling 5000 points at random from the images. The training was performed on 100 000 epochs and converged with the error E of 0.018. Then, a method for designing the structure of the NF in [50]–[52] was applied to the trained NF. The optimal structure, which is the smallest structure with this error, was obtained: The number of units in the input and hidden layers became 22 and 8, respectively.

Fig. 15. Comparison of image quality between the output image of the NF trained to reduce quantum noise in natural images and that of its approximate filter. (a) Noisy input image. (b) Teaching image. (c) Output image of the trained NF. (d) Output image of the approximate filter.

The output images of the trained NF and its approximate filter are shown in Fig. 15(c) and (d), respectively. The ISNRs of the NF and the approximate filter are 7.564 and 7.699 dB, respectively. Furthermore, in order to evaluate the generalization ability, these filters were applied to the test images that are not used for training. The output images of the filters in filtering the test images are shown in Fig. 16. The results of calculation of the ISNRs are shown in Table II. The ISNRs of the approximate filter are slightly better than those of the NF. The output responses of the NF were slightly saturated, like those shown in Fig. 5. They were approximated by linear functions. This approximation makes the gain of the approximate filter higher, particularly at the saturated parts. By this effect, the contrast of the image was improved. This is the reason the ISNRs of the approximate filter are better. These results demonstrate that the proposed analysis method and the approximate filter function well in approximation of the NF trained with natural images.

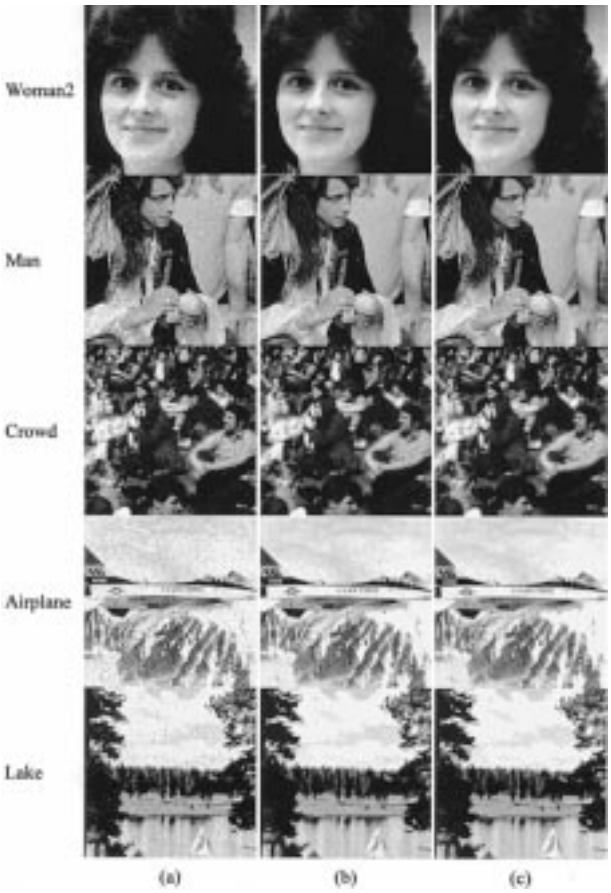

Fig. 16. Comparison of image quality between the output image of the trained NF and that of its approximate filter in filtering test images. (a) Noisy input images. (b) Output images of the trained NF. (c) Output images of the approximate filter.

TABLE II
QUANTITATIVE EVALUATION OF THE ACCURACY IN APPROXIMATION BETWEEN THE TRAINED NF AND ITS APPROXIMATE FILTER

		ISNR [dB]	
Image	BSNR [dB]	Neural filter	Approximate filter
Woman2	13.2	8.3	8.3
Man	10.9	4.1	4.5
Crowd	12.5	3.2	3.5
Airplane	8.7	6.3	6.6
Lake	13.2	3.9	4.2

V. CONCLUSIONS

In this paper, a novel method for analyzing the NFs for removing quantum noise from images has been proposed. The experiments to analyze the NFs trained to remove quantum noise from medical X-ray image sequences and natural images were performed. The proposed method has been proved to be useful to analyze unknown nonlinear deterministic systems with plural inputs such as the trained NFs. The results of the analysis of the trained NFs made the characteristics clear, leading to their efficient approximate filters. The experimental results demonstrated that the approximate filters, constructed of simple hardware, are sufficient for approximation of the trained NFs and efficient at computational cost.

The problem of filtering Poisson noise can be simplified to a case of filtering invariant Gaussian noise by means of a squire-root operation, the form of which is the following: $\sqrt{g_L(x,y,t)+c}$, where c is a constant. By applying the square-root operation to a signal with Poisson noise, we can obtain a signal with a constant noise variance, i.e., the signal-dependent quantum noise becomes signal-independent additive noise after the square-root operation [53]. Using this operation prior to filtering, we may be able to obtain a simpler implementation of the approximate filter for medical images. We will perform the experiment to investigate the effectiveness of this operation prior to filtering.

We plan in the near future to study the the extension of the proposed analysis method so that NNs trained to solve various problems, e.g., various kinds of NN models such as radial basis function networks, etc., can be handled. We will perform the mathematical analyses on the statistical properties of the quantum noise and on the removal of noise using NNs.

ACKNOWLEDGMENT

The authors wish to thank K. Koike, Dr. K. Ishikawa, S. Ikeda, K. Suzuki, and S. Sugeno of Hitachi Medical Corporation for their valuable suggestions and cooperation, Vice President M. Nanki, M.D. and clinical staffs of Chubu Rosai Hospital for evaluating images and cooperating with experiments, and Dr. K. Ueda of Nagoya Electric Works and Prof. S. Yamamoto of Meijo University for their constructive suggestions. The authors also thank anonymous reviewers for their valuable comments.

REFERENCES

[1] P. D. Wendt, E. J. Coyle, and N. C. Gallagher, Jr., "Stack filters," *IEEE Trans. Acoust., Speech, Signal Processing*, vol. ASSP-34, pp. 898–911, 1986.
[2] L. Yin, J. Astola, and Y. Neuvo, "Adaptive neural filters," in *Proc. IEEE Int. Workshop Neural Networks Signal Process.*, Sept. 1991, pp. 503–512.
[3] A. Asano, K. Itoh, and Y. Ichioka, "Optimization of the weighted median filter by learning," *Opt. Lett.*, vol. 16, no. 3, pp. 168–170, Feb. 1991.
[4] L. Yin, J. Astola, and Y. Neuvo, "Neural filters: A class of filters unifying FIR and median filters," in *Proc. IEEE Int. Conf. Acoust., Speech, Signal Process.*, Mar. 1992, pp. 53–56.
[5] ——, "A new class of nonlinear filters—Neural filters," *IEEE Trans. Signal Processing*, vol. 41, pp. 1201–1222, Mar. 1993.
[6] H. Hanek, N. Ansari, and Z. Z. Zhang, "Comparative study on the generalized adaptive neural filter with the other nonlinear filter," in *Proc. IEEE Int. Conf. Acoust., Speech, Signal Process.*, vol. I, Minneapolis, MN, Apr. 1993, pp. 649–652.
[7] L. Yin, J. Astola, and Y. Neuvo, "Adaptive multistage weighted order statistic filters based on the back propagation algorithm," *IEEE Trans. Signal Processing*, vol. 42, pp. 419–422, Feb. 1994.
[8] N. Ansari and Z. Z. Zhang, "Generalized adaptive neural filters," *Electron. Lett.*, vol. 20, no. 4, pp. 342–343, Feb. 1994.
[9] Z. Z. Zhang and N. Ansari, "Structure and properties of generalized adaptive neural filters for signal enhancement," *IEEE Trans. Neural Networks*, vol. 7, pp. 857–868, July 1996.
[10] H. Hanek and N. Ansari, "Speeding up the generalized adaptive neural filters," *IEEE Trans. Image Processing*, vol. 5, pp. 705–712, May 1996.
[11] K. Arakawa and H. Harashima, "A nonlinear digital filter using multilayered neural networks," in *Proc. IEEE Int. Conf. Commun.*, vol. 2, 1990, pp. 424–428.
[12] ——, "Design of layered-neural nonlinear filters using back-propagation algorithm," *Trans. IEICE A*, vol. J74-A, no. 3, pp. 421–429, Mar. 1991.

[13] K. Suzuki, I. Horiba, N. Sugie, and S. Ikeda, "Improvement of image quality of X-ray fluoroscopy using spatiotemporal neural filter which learns noise reduction and edge enhancement," in *Proc. Int. Conf. Signal Process. Applicat. Technol.*, vol. 2, Boston, MA, Oct. 1996, pp. 1382–1386.
[14] K. Suzuki, I. Horiba, N. Sugie, and M. Nanki, "A recurrent neural filter for reducing noise in medical X-ray image sequences," in *Proc. Int. Conf. Neural Inform. Process.*, vol. 1, Kitakyushu, Japan, Oct. 1998, pp. 157–160.
[15] ——, "Noise reduction of medical X-ray image sequences using a neural filter with spatiotemporal inputs," in *Proc. Int. Symp. Noise Reduction Imag. Commun. Syst.*, Tokyo, Japan, Nov. 1998, pp. 85–90.
[16] K. Suzuki, I. Horiba, and N. Sugie, "Signal-preserving training for neural networks for signal processing," in *Proc. IEEE Int. Symp. Intell. Signal Process. Commun. Syst.*, vol. 1, Honolulu, HI, Nov. 2000, pp. 292–297.
[17] ——, "Neural filter with selection of input features and its application to image quality improvement of medical image sequences," in *Proc. IEEE Int. Symp. Intell. Signal Process. Commun. Syst.*, vol. 2, Honolulu, HI, Nov. 2000, pp. 783–788.
[18] ——, "Training under achievement quotient criterion," in *Proc. IEEE Int. Workshop Neural Networks Signal Process. X*, B. Widrow *et al.*, Eds., Sydney, Australia, Dec. 2000, pp. 537–546.
[19] E. J. Coyle and N. C. Callagher, "Stack filters and neural networks," in *Proc. Int. Symp. Circuits Syst.*, Portland, OR, 1989, pp. 975–978.
[20] P. T. Yu and E. J. Coyle, "The classification and associative memory capability of stack filters," *IEEE Trans. Signal Processing*, vol. 40, pp. 2483–2497, Oct. 1992.
[21] K. Funahashi, "On the approximate realization of continuous mappings by neural networks," *Neural Networks*, vol. 2, pp. 183–192, 1989.
[22] A. R. Barron, "Universal approximation bounds for superpositions of a sigmoidal function," *IEEE Trans. Inform. Theory*, vol. 39, pp. 930–945, Mar. 1993.
[23] G. Cybenko, "Approximation by superpositions of a sigmoidal function," *Math. Contr., Signals, Syst.*, vol. 2, pp. 303–314, 1989.
[24] K. Funahashi, "On the approximate realization of continuous mappings by neural networks," in *Proc. Int. Joint. Conf. Neural Networks*, vol. I, 1988, pp. 614–648.
[25] K. M. Hornik, M. Stinchcombe, and H. White, "Multilayer feedforward networks are universal approximators," *Neural Networks*, vol. 2, pp. 359–366, 1989.
[26] K. M. Hornik, "Approximation capabilities of multilayer feedforward networks are universal," *Neural Networks*, vol. 4, no. 2, pp. 251–257, 1991.
[27] K. Ueda, M. Yamada, I. Horiba, K. Ikegaya, and K. Suzuki, "A direct estimation method of occupancy rate in parking lot using analogue output neural network model," *Trans. IPSJ*, vol. 36, no. 3, pp. 627–635, Mar. 1995.
[28] K. Suzuki, I. Horiba, N. Sugie, and M. Nanki, "Computer-aided diagnosis system for coronary artery stenosis using a neural network," *Proc. SPIE Med. Imag.: Image Process.*, vol. 4322, pp. 1771–1782, June 2001.
[29] D. E. Rumelhart, G. E. Hinton, and R. J. Williams, *Learning Internal Representations by Error Propagation*. Cambridge, MA: MIT Press, 1986, vol. 1, ch. 8, pp. 318–362.
[30] A. Macovski, *Medical Imaging Systems*. Englewood Cliffs, NJ: Prentice-Hall, 1983.
[31] T. Aach, U. W. Schiebel, and G. Spekowius, "Digital image acquisition and processing in medical X-ray imaging," *J. Electron. Imag.*, vol. 8, no. 1, pp. 7–22, Jan. 1999.
[32] T. Aach and D. Kunz, "Spectral estimation filters for noise reduction in X-ray fluoroscopy imaging," in *Proc. EUSIPCO*, Sept. 1996, pp. 571–574.
[33] R. Aufrichtig, P. Xue, C. W. Thomas, G. C. Gilmore, and D. L. Wilson, "Perceptual comparison of pulsed and continuous fluoroscopy," *Med. Phys.*, vol. 21, pp. 245–256, 1994.
[34] N. Tsoulfanidis, *Measurement and Detection of Radiation*. Washington, DC: Hemisphere, 1983, pp. 34–43.
[35] F. Takahashi, K. Ishikawa, and T. Taniguchi *et al.*, "Development of a high definition real-time digital radiography system using a 4 million pixels CCD camera," in *Proc. SPIE Med. Imag.*, vol. 3032, Feb. 1997, pp. 364–375.
[36] K. Suzuki, I. Horiba, and N. Sugie, "Efficient approximation of a neural filter for quantum noise removal in X-ray images," in *Proc. IEEE Int. Workshop Neural Networks Signal Process. IX*, Y.-H. Hu, Ed., Madison, WI, Aug. 1999, pp. 370–379.
[37] M. R. Banham and A. K. Katsaggelos, "Digital image restoration," *IEEE Signal Processing Mag.*, vol. 14, pp. 24–41, Mar. 1997.
[38] J. C. Brailean, R. P. Kleihorst, S. Efstratiadis, A. K. Katsaggelos, and R. L. Lagendijk, "Noise reduction filters for dynamic image sequences: A review," *Proc. IEEE*, vol. 83, pp. 1270–1291, Sept. 1995.
[39] R. A. Kruger, "A method for time-domain filtering using computerized fluoroscopy," *Med. Phys.*, vol. 8, pp. 466–470, 1981.
[40] S. J. Riederer, A. L. Hall, J. K. Maier, N. J. Pelc, and D. R. Enzmann, "The technical characteristics of matched filtering in digital subtraction angiography," *Med. Phys.*, vol. 10, pp. 209–217, 1983.
[41] C. W. Hardin, R. A. Kruger, F. L. Anderson, B. E. Bray, and J. A. Nelson, "Real-time digital angiocardiography using a temporal high-pass filter," *Radiol.*, vol. 151, pp. 517–520, 1984.
[42] M. K. Ozkan, A. T. Erdem, M. I. Sezan, and A. M. Tekalp, "Efficient multiframe Wiener restoration of blurred and noisy image sequences," *IEEE Trans. Image Processing*, vol. 1, pp. 453–476, Oct. 1992.
[43] M. K. Ozkan, M. I. Sezan, and A. M. Tekalp, "Adaptive motion-compensated filtering of noisy image sequences," *IEEE Trans. Circuits Syst. Video Technol.*, vol. 3, pp. 277–290, Aug. 1993.
[44] K. Enomoto, T. Hayashi, I. Horiba, I. Ikegaya, and M. Nanki, "Improving image quality of X-ray fluoroscopy," in *Proc. Tokai-Sec. Joint Conf. Seven Inst. Elect. Relat. Eng.*, 1993, p. 731.
[45] E. W. Edmonds, J. A. Rowlands, D. M. Hynes, B. D. Toth, and A. J. Porter, "Digital methods for reducing exposure during medical fluoroscopy," in *Proc. SPIE Med. Imag.*, vol. 1450, 1990, pp. 406–411.
[46] C. L. Chan, B. J. Sullivan, A. V. Sahakian, A. K. Katsaggelos, T. Frohlich, and E. Byrom, "Spatio-temporal filtering of digital angiographic image sequences corrupted by quantum mottle," in *Proc. SPIE Biomed. Imag. Process. II*, vol. 1450, 1991, pp. 208–217.
[47] C. L. Chan, A. K. Katsaggelos, and A. V. Sahakian, "Image sequence filtering in quantum-limited noise with applications to low-dose fluoroscopy," *IEEE Trans. Med. Imag.*, vol. 12, pp. 610–621, Mar. 1993.
[48] R. Aufrichtig and D. L. Wilson, "X-ray fluoroscopy spatio-temporal filtering with object detection," *IEEE Trans. Med. Imag.*, vol. 14, pp. 733–746, Apr. 1995.
[49] M. L. Giger, K. Doi, and H. Hujita, "Noise Wiener spectra of I.I.-TV digital imaging systems," *Med. Phys.*, vol. 13, pp. 131–138, Mar. 1986.
[50] K. Suzuki, I. Horiba, and N. Sugie, "Designing the optimal structure of a neural filter," in *Proc. IEEE Int. Workshop Neural Networks Signal Process. VIII*, M. Niranjan, Ed., Cambridge, U.K., Aug. 1998, pp. 323–332.
[51] ——, "An approach to synthesize filters with reduced structures using a neural network," in *Quantum Information II*, T. Hida and K. Saito, Eds, Singapore: World Scientific, 2000, pp. 205–218.
[52] ——, "A simple neural network pruning algorithm with application to filter synthesis," *Neural Process. Lett.*, vol. 13, no. 1, pp. 43–53, Feb. 2001.
[53] F. J. Anscombe, "The transformation of poisson, binomial and negative-binomial data," *Biometrica*, vol. 35, pp. 246–254, 1948.

Kenji Suzuki (M'96) was born in Nagoya, Japan, in 1968. He received the B.S. and M.S. degrees, both with highest honors, in electrical and electronic engineering from Meijo University, Nagoya, in 1991 and 1993, respectively, and the Ph.D. degree in information engineering by a thesis from Nagoya University in 2001.

From 1993 to 1997, he was with the Research and Development Center at Hitachi Medical Corporation, Kashiwa, Japan, as a Researcher. He was engaged in research and development of intelligent medical imaging systems, including a digital subtraction angiography system and a digital radiography system. In 1997, he joined Aichi Prefectural University, Aichi, Japan, where he assisted in founding the Faculty of Information Science and Technology. He has been a Research Associate with the Faculty of Information Science and Technology at Aichi Prefectural University since 1998. Since 2001, he has been a Visiting Research Associate with the Kurt Rossmann Laboratories for Radiologic Image Research, the Department of Radiology, the Division of Biological Sciences, the University of Chicago, Chicago. IL. He was a member of the research group organized by the Aichi Science and Technology Foundation of Japan from 1997 to 1998. He has been a member of the research project promoted by the Ministry of Education, Science, Sports, and Culture of Japan, Quantum Information Theoretical Approach to Life Science, in the Frontiers of Science and Technology at Meijo University since 1997. His research interests include neural networks for image processing and pattern recognition, generalization issues, and image processing suggested by the human visual systems.

Dr. Suzuki is a member of IEICE, IEEJ, IPSJ, JNNS, and JCS.

Isao Horiba was born in Nagoya, Japan, in 1948. He received the B.S. and Ph.D. degrees in electrical engineering from Nagoya University in 1974 and 1985, respectively.

From 1974 to 1987, he was with the Research and Development Center at Hitachi Medical Corporation, Kashiwa, Japan, as a Senior Researcher. He was engaged in the development of computed topography systems and in research and development of many kinds of medical imaging systems, including magnetic resonance imaging systems, digital subtraction angiography systems, digital radiography systems, and so on. In 1987, he joined the Faculty of Science and Technology at Meijo University, Nagoya, as an Assistant Professor and then as an Associate Professor. He has been a Professor with the Faculty of Information Science and Technology at Aichi Prefectural University, Aichi, Japan, since 1998. He has published more than 50 papers and is co-author of three books in the area of medical engineering and image understanding for intelligent transportation systems. He has been a member of the research project promoted by the Ministry of Education, Science, Sports , and Culture of Japan, Quantum Information Theoretical Approach to Life Science, in the Frontiers of Science and Technology at Meijo University since 1997. His research interests include intelligent image processing, image processing for medical systems, and image understanding for intelligent transportation systems.

Prof. Horiba received the Best Technology Award from the Japan Society of Medical Electronics and Biological Engineering and the Best Patent Award from the Japan Institute of Invention and Innovation in 1988 and 1990, respectively. He was a Senator of the IPSJ from 1997 to 1999. He has been a member of the Technical Committee of IEEJ since 1990. He is a member of IEICE, IPSJ, JSMIT, JSUM, and JMEBE.

Noboru Sugie (M'85) was born in Nagoya, Japan, in 1932. He received the B.S. degree in electrical engineering from Nagoya University in 1957 and the Ph.D. degree in engineering from the University of Tokyo, Tokyo, Japan, in 1970.

From 1957 to 1979, he was with the Government Electrotechnical Laboratory, Tsukuba, Japan. From 1962 to 1964, he was on leave with the Department of Electrical Engineering, McGill University, Montreal, QC, Canada as an NRC Postdoctoral Fellow. He had been the Director of the section of bionics and vision at the Government Electrotechnical Laboratory from 1970 to 1978. From 1979 to 1994, he was a Professor with the Department of Information Engineering and the Graduate School of Engineering at Nagoya University. From 1990 to 1994, he was the Director of the Nagoya University Computation Center. He is now a Professor Emeritus of Nagoya University. From 1994 to 2000, he was a Professor with the Department of Electrical and Electronic Engineering and the Graduate School of Science and Technology at Meijo University, Nagoya. Since 2000, he has been the Founding Chairman of the Department of Information Sciences. He has published more than 300 papers and is author or editor of more than 50 books in the area of computer vision, human vision, biocybernetics, and natural language processing. He has served as an editor of many journals and as a member of organizing committees of many international conferences. His research interests include computer vision, human vision, biocybernetics, and natural language processing.

Prof. Sugie received the Technological Achievement Award from the Society of Instrument and Control Engineers in 1996. He was an Executive Director of the Japanese Society for AI, the Japan Society for Simulation Technology and Society of Biomechanisms Japan, a Director of IPSJ and ITE, an advisor to JMEBE and the Japanese Neural Network Society, and a Senator of IEICE and the Robotics Society of Japan.